

# Optimum Driving a Z-Pinch for Soft X-Ray Lasers

H. Ghomi<sup>a,\*</sup>, M. Yousefi<sup>a</sup>, SH. Rostami<sup>a</sup>, Y. Hayashi<sup>b</sup>, and E. Hotta<sup>b</sup>

<sup>a</sup>Laser Research Institute of Shahid Beheshti University, Evin 1983963113, Tehran, Iran.

<sup>b</sup>Department of Energy Sciences, Tokyo Institute of Technology, 4259 Nagatsuta, Midori-ku, Yokohama 226-8502, Japan

\*Corresponding Author Email: [H-GMDashty@cc.sbu.ac.ir](mailto:H-GMDashty@cc.sbu.ac.ir)

**Abstract**— A z-pinch capillary plasma as an alternative active medium of soft X-Ray lasers was studied experimentally and theoretically. The theoretical analysis was based on the self consistent solution of the so called “snow plow” model. The dynamics of pinched plasma is determined by the capillary parameters and by the time dependence of electrical current passing through it. The current time dependence is strongly influenced by the electrical circuit connected to the capillary. In order to optimize the pinch dynamics from the point of view of laser pumping, the effects of the electrical circuit parameters on plasma evolution are studied in this paper.

**KEYWORDS:** z-pinch, x-ray lasers, capillary plasma, azimuthally magnetic field, pinch time, RLC pumping circuit.

## I. INTRODUCTION

“Z-pinch” is a simple plasma configuration in which a longitudinal current induces a magnetic field that tends to confine the plasma [1-3]. The simple geometry and low cost, made Z-pinch an appropriate candidate for soft x-ray sources and controlled fusion [4]. The soft x-ray has a lot of application in other field of science and industry. These applications are microscopy, holography, diagnostic of dense plasma, and the excitation of nonlinear photo luminescence in crystals [5-11]. Initial conductive plasma, created by wall ablation or gas ionization, fills the capillary. Increasing external voltage in the first quarter period causes a quick increase of axial electric current inside the capillary, inducing azimuthally magnetic field,  $B$ . The azimuthally magnetic

field and axial current make a  $\mathbf{J} \times \mathbf{B}$  force. The force pushes the current sheet to contract laterally (into the axis), which is known as pinch effect. In the pinch effect (up to pinch time), the Lorentz force is stronger than gas kinetic pressure. But after the pinch time, the gas kinetic pressure inside the current sheet becomes more than the Lorentz force and the current sheet expanded to the wall [12, 13].

In Z-pinch experiment estimation and detection of pinch time is very important. Usually, the pinch time occurs sooner than the current peak at first quarter of current period which brings about lots of electrical energy dissipation in the capillary after the pinch time. This time is stimulated through a simple model, which is called “snow plow” model. Although it is not a complete model, the results related to the pinch time, are confirmed with the experimental data [12-14].

The effect of initial conditions such as pressure, current amplitude and period or tube radii can be calculated through snow plow model. In our previous investigations, approximate conditions of the gas pressure and discharge current for a giving pinch time were derived to control the lasing time and improve the energy conversion efficiency. Also the gain characteristics of Ne-like Ar soft X-ray laser, by changing the plasma length and the gas pressure were studied. A quantity of “the gain-length product at the pressure of maximum laser output” was suggested for comparing the amplification capability of soft X-ray laser devices, which use capillary discharge [15-17].

As it was said, we want to minimize the time interval between the pinch time and current peak, to reduce the energy dissipation. The useful parameter for these calculations is an output efficiency which is defined as the ratio of the final kinetic energy of the current sheet, to the energy that the electrical pumping circuit could deliver to the capillary [17].

In this paper, effects of capacitance, inductance and resistance of external circuit on the pinch time and also electrical efficiency of a Z-pinch machine were studied. Also the calculated pinch time is compared with different experimental reports.

## II. THEORETICAL CONSIDERATIONS

In this context we have developed the high charging voltage (400 kV) fast electrical z-pinch discharge that was filled by argon to a selected pressure in the region (13-133 Pa) for the production of pulses of intense soft x-ray radiation in the spectral region of 2-50 nm. The effect of the electrical circuit parameters on plasma evolution and efficiency of the output beam are studied for current pulses of amplitude from (20-40 kA) and a half cycle duration of (110 ns).

The capillary was placed in the axis of a 3nF liquid-dielectric capacitor. The capacitor was pulse-charged by a 3-stage Marx generator and a transformer. The impedance of the capacitor is 5.5 Ohm. The capillary loads were excited by discharging the capacitor through a spark gap switch, pressurized with SF<sub>6</sub> (1atm) [14-16].

In the actual situations, the inductance and resistance arising from various sources such as the capacitors, transmission lines, switches, plasma capillary and etc.

So the equivalent circuit of our pumping system should be represented approximately by a RLC series circuit (Fig. 1). Presuming that R and L are time independent, (neglecting the inductance and resistance of the capillary) the pinch evolution is determined by simultaneous solution of its dynamic and

equivalent external pumping circuit equations [10]:

$$\frac{dr(t)}{dt} = V(t) \quad (1)$$

$$\frac{d}{dt} \left[ \pi \rho_0 (a^2 - r^2) \frac{dr}{dt} \right] = \begin{cases} 0 & 0 < t < t_s \\ -\frac{\mu_0 I^2(t)}{4\pi r} + 2\pi r P_{in} & t_s < t \end{cases} \quad (2)$$

$$\frac{dU}{dt} = -\frac{I(t)}{C} \quad (3)$$

$$\frac{dI(t)}{dt} = \frac{U(t) - RI(t)}{L} \quad (4)$$

First equation shows the radial velocity of the particles in the moving sheet and its relation to the instantaneous sheet position  $r(t)$ . Momentum conservation law and Bennett's condition for starting the compression impose the second equation. Assuming a simple RLC circuit for the discharge pumping, comes to the other two equations.

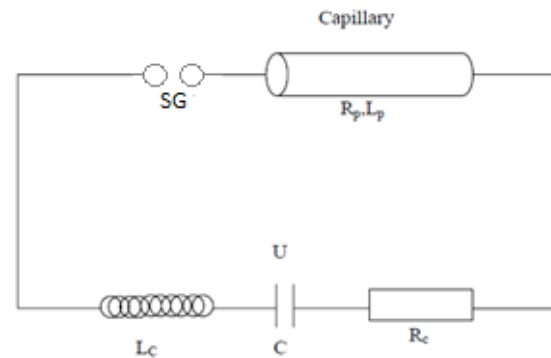


**Fig. 1:** RLC pumping circuit

This set of equations, are normalized to be solved. Introducing normalized time  $\tau = t/t_1$ , plasma sheet position  $\chi = r/a$ , sheet velocity  $v = a/t_1 V$ , current  $I' = I/I_1$  and the voltage  $\eta = U/U_0$  change the set of equations (1)-(4) to the following forms [10]:

$$\frac{d\chi(\tau)}{d\tau} = v(\tau) \quad (5)$$

$$\frac{d}{d\tau}[(1-\chi^2(\tau))v(\tau)] = \begin{cases} 0 & 0 < \tau < \tau_s \\ -\frac{I'^2(\tau)}{\chi(\tau)} + \alpha\chi^{-7/3} & \tau_s < \tau \end{cases} \quad (6)$$

$$\frac{d\eta(\tau)}{d\tau} = -\beta I'(\tau) \quad (7)$$

$$\frac{dI'(\tau)}{d\tau} = \eta(\tau) - \gamma I'(\tau) \quad (8)$$

The initial condition (at  $t=0$ ) are:  $V(0)=0$  speed of the current sheet,  $r(0)=a$  sheet position,  $I(0)=0$  loop current,  $U(0)=U_0$  capacitor voltage.

The characteristic time  $t_1$ , characteristic current  $I_1$  and three dimensionless parameters  $\alpha$ ,  $\beta$ , and  $\gamma$  are defined as:

$$t_1 = \left[ \frac{2aL}{\eta_0} \sqrt{\frac{\pi}{\mu_0}} \right]^{1/2} M_0^{1/4} \quad (9)$$

$$I_1 = \frac{U_0 t_1}{L} \quad (10)$$

$$\alpha = \frac{4\pi}{\sqrt{\mu_0 \rho_0}} \frac{P_0 L}{\eta_0} \quad (11)$$

$$\beta = \frac{t_1^2}{LC} \quad (12)$$

$$\gamma = \frac{R t_1}{L} \quad (13)$$

where  $M_0 = \pi \rho_0 a^2$  is the mass of plasma on unit length. The solutions of Eqs. (5)-(8) indicate the pinch dynamic behavior.

### III. RESULTS AND DISCUSSIONS

First of all, we examine the correctness of our program and the result of the numerical calculations. The comparison between experimental data and the numerical results are given in Table 1. Table 1 presents experimental and theoretical values of pinch time for different conditions. The pressure changes from 39 to 80 Pa, current amplitude has different values such as 25, 30 and 32 kA, for two sizes of capillary radius 2.5 and 1.5

mm also current period has three values, 340, 220 and 180 ns. As it is obvious, there is an acceptable agreement between the computational results and experimental ones, so one can trust on the results of numerical calculations.

As it is shown in Fig. 2 the time  $t_s$  indicates the plasma separation from the capillary wall and the minimum pinch radius is reached at pinch time ( $t_p \approx 31$  ns), where the sign of sheet velocity which shows the direction of plasma sheet moving, changes abruptly. In the next stage ( $t > t_{pinch}$ ) the plasma sheet expansion and the broken pinch can be seen.

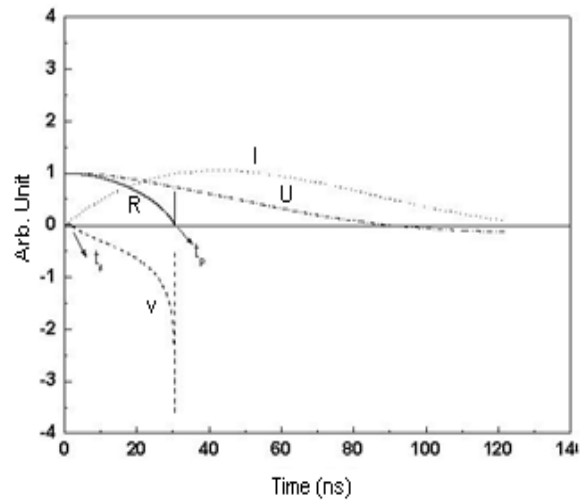


**Fig. 2:** Time dependencies of normalized radius  $\chi$ , velocity  $v$ , current  $I'$  and voltage  $\eta$  for  $\alpha = 1.5748 \times 10^5$ ,  $\beta = 0.2543$ , and  $\gamma = 0.5401$  (Voltage=400 kV, current peak=32 kA, period=220 ns Capillary radius=1.5 mm)

Table 1 presents the pinch time for different experimental measurement. It is shown that, by decreasing the current period pinch time decreases such that, at 340 ns current period the pinch was measured about 90 ns, but at 220 ns current period, the pinch decreases to 44 ns. On the other hand, we calculate pinch time for different condition and we find about 10 % differences between experiment and our calculation. It is easy to see that, in case 1 the calculated pinch time is 83 ns but experiment finds it about 90 ns. Please note that, by decreasing the current period the difference between calculation and experiment on pinch time decreases.

Table 1. Experimental and calculated results of pinch dynamic in different conditions.

| Quantity | Capillary radius (mm) | Pressure (pa) | Current amplitude (Amp) | Current period (ns) | Experimental pinch time $\pm 1$ (ns) | Calculated pinch time (ns) |
|----------|-----------------------|---------------|-------------------------|---------------------|--------------------------------------|----------------------------|
| 1        | 2.5                   | 66.5          | 25000                   | 340                 | 90 [11]                              | 83                         |
| 2        | 2.5                   | 66.5          | 30000                   | 180                 | 60 [11]                              | 64                         |
| 3        | 2.5                   | 53.2          | 30000                   | 180                 | 53 [11]                              | 58                         |
| 4        | 1.5                   | 39.9          | 32000                   | 220                 | 35 [15]                              | 30                         |
| 5        | 1.5                   | 53.2          | 32000                   | 220                 | 37 [15]                              | 33                         |
| 6        | 1.5                   | 59.85         | 32000                   | 220                 | 38 [15]                              | 34                         |
| 7        | 1.5                   | 66.5          | 32000                   | 220                 | 40 [15]                              | 35                         |
| 8        | 1.5                   | 73.15         | 32000                   | 220                 | 41 [15]                              | 36                         |
| 9        | 1.5                   | 79.8          | 32000                   | 220                 | 42 [15]                              | 37                         |
| 10       | 1.5                   | 93.1          | 32000                   | 220                 | 43 [15]                              | 39                         |
| 11       | 1.5                   | 99.75         | 32000                   | 220                 | 44 [15]                              | 40                         |

The parameters  $\alpha$  and  $\gamma$  show the dependency of the plasma column compression on the inductance. As it is known depending on the relative magnitudes of  $R$ ,  $L$ , and  $C$  values, for  $R < 2(L/C)^{1/2}$  (which is usually the case) the current,  $i$  in the circuit may be written as [10]:

$$i = i_0 \exp(-\zeta t) \sin \omega t. \quad (14)$$

From Eq. (14), it can be seen that, regardless of what values for other parameters, the maximum rate of current increase is inversely proportional to  $L$ . That is, the smaller the  $L$  the faster the current rise time.

$$\left(\frac{di}{dt}\right)_m \approx U_0/L, \quad (15)$$

where  $\zeta = \frac{R}{2L}$ ,  $\omega = \left[\frac{1}{LC} - \frac{R^2}{4L^2}\right]^{1/2}$ , and  $i_0 = \left[\frac{(\omega^2 + \zeta^2)}{\omega}\right]CU_0$ .

Therefore, for fast pulses it is always desired to keep the inductance of the circuit minimal. This fact refers to variable current period and it means that the current will reach to its maximum value in a smaller time. Figure 3 shows the dependency of efficiency  $\left(\frac{(MIV^2/2)}{(CU^2/2)}\right)$ , which is defined as the kinetic energy of the plasma current sheet at the end of the implosion (just right before pinch) divided by the total energy stored in the capacitor [17], and pinch time to the normalized value of inductance. As it was explained, we are searching for optimum

conditions, so regarding to Fig. 3(b) for having the pinch effect near the current peak (to reduce the energy dissipation) we should reduce the inductance. As a matter of fact, when the current sheet, implodes with a higher speed, the pinch time decreases, which is in agreement with our numerical calculation results (Figs. 3(a) and (b)). Figure 4 is an evidence for this procedure.

There are several ways that may reduce the inductance of the system, and getting more energy and efficiency, for instance, using low inductance capacitor, selecting proper dimensions for transmission lines and load and so on.

If we want to examine the role of the other parts of the pumping system in the efficiency and pinch time, the importance of the water capacitor can't be neglected. As a rule when we use the higher capacitance in our pumping setup, it will deposit more energy on the capillary through its discharge and creates higher current and so higher induced magnetic field. As a result, grater force pushes the plasma sheet inwardly and the sheet is compressed faster, so we can have the laser beam sooner. In this case also we get higher energy and efficiency

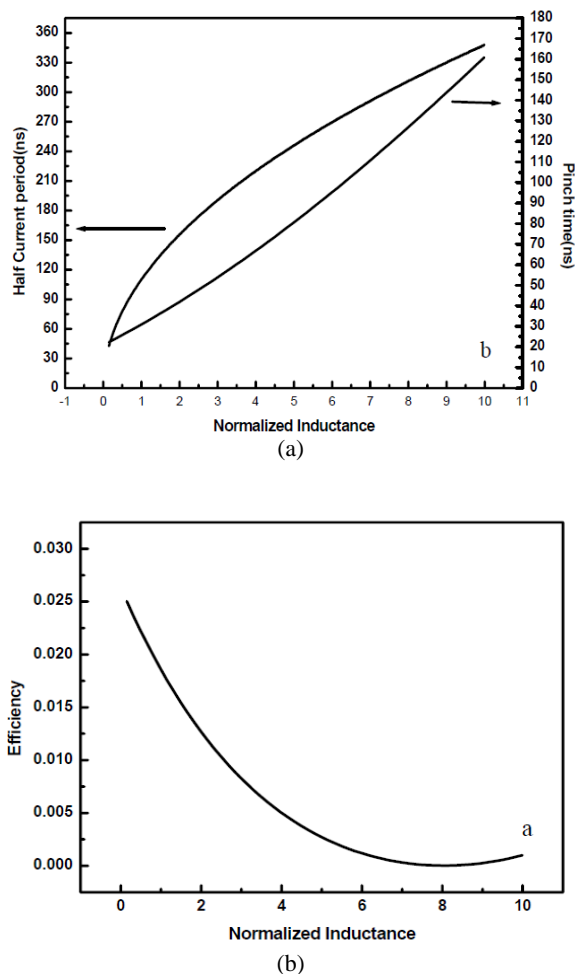


**Fig. 3:** Dependencies of (a) efficiency and (b) pinch time and Half Current period on Normalized Inductance,  $\sigma$ , for  $\alpha = 1.5748 \times 10^{-5} \sigma$ ,  $\beta = 0.2543$ ,  $\gamma = 0.5401 / \sqrt{\sigma}$  (Voltage=400 kV, Current peak=32 kA, Current period=220 ns, Capillary radius=1.5 mm)

As it was shown in Fig. 4 (a), efficiency has a maximum value around  $\kappa = 0.4$  and then decreases as a function of normalized capacitance. Decreasing part of the curve defines, faster increase of the denominator which refers to the electrical energy that is stored in the water capacitor ( $CU^2/2$ ) comparing to the kinetic energy of the plasma sheet ( $M_0 l V^2/2$ , where  $l$  is the capillary length), which is placed as a nominator, pinch energy rises and then remains almost constant. So for optimizing the efficiency, we should select the normalized capacitance in the region  $\kappa = 0.2 - 0.7$ . Likewise we can see the pinch time decreasing with higher capacitances in Fig. 4(b). So we should select the right value

for the pumping capacitor to reduce the delay time between the pinch time and peak current, in smaller region of capacitances. For example, at  $\kappa = 0.4$  the current period will be about 140 ns ( $T/4 = 34.8$  ns) and the pinch occurs at 32.1 ns. This means that, the pinch occurs in the vicinity of the first current peak.

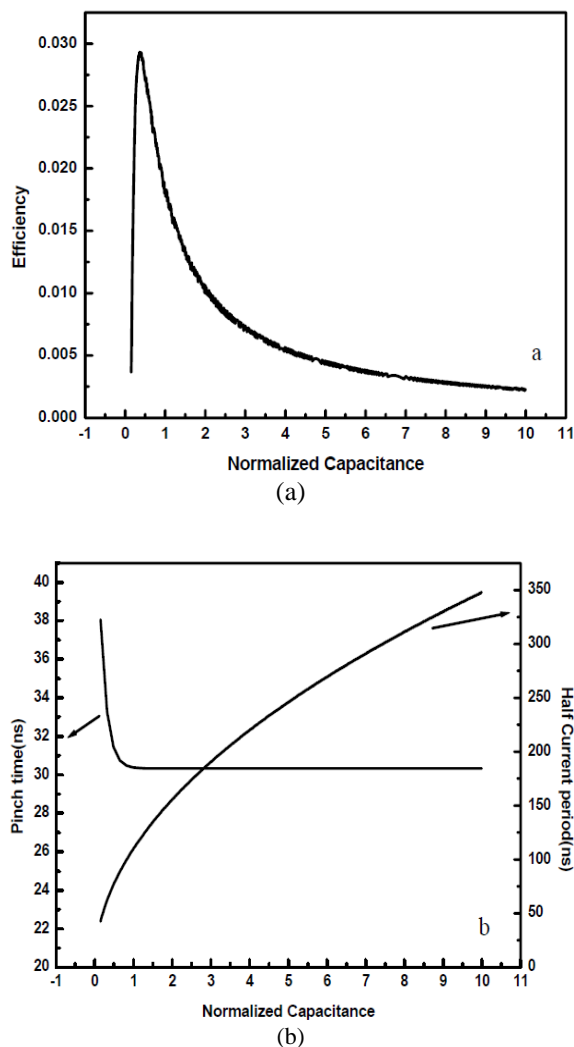


**Fig. 4:** Dependencies of (a) efficiency and (b) pinch time and half current period on normalized capacitance  $\kappa$  for  $\alpha = 1.5748 \times 10^{-5}$ ,  $\beta = 0.2543 / \kappa$ , and  $\gamma = 0.5401$

If  $\alpha$  and  $\beta$ , are considered as an invariable parameters and  $\gamma$  changes as a linear function of the circuit resistance, with helping of the computational programs, the effect of pumping resistance will be taken into account. Obviously we anticipate a decreasing approach for plasma sheet energy, because grater

resistance causes grater current damping, so it leads to weaker magnetic pressure and slower compression.

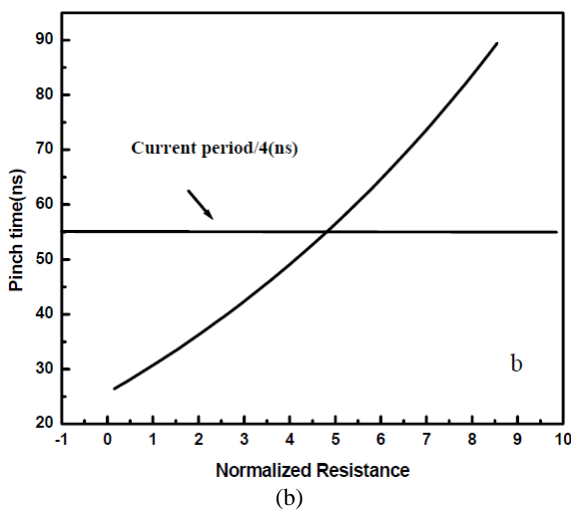
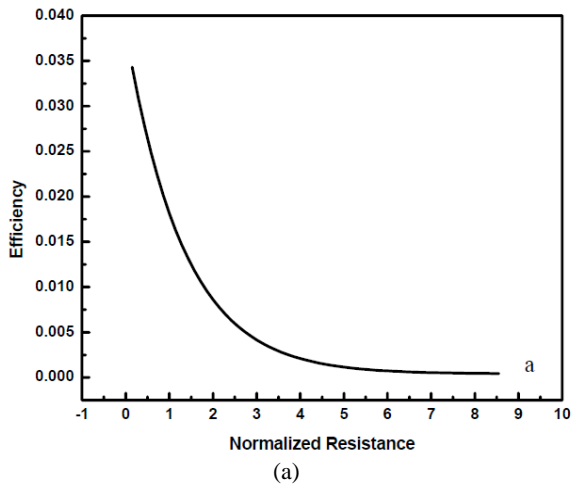


**Fig. 5:** Normalized resistance dependencies  $r'$ , of (a) efficiency and (b) pinch time and current period/4, for  $\alpha = 1.5748 \times 10^{-5}$ ,  $\beta = 0.2543$ , and  $\gamma = 0.5401r'$ .

It was expected, Fig. 5 shows, if we reduce the resistance of the pumping circuit we'll get more kinetic energy and we can have the laser pulse, sooner. Although, it was said that for maximum efficiency, we have to choose the parameters in a way that the pinch happens as near as possible to the peak current, this postulation is not correct in this case. Choosing the value of normalized resistance between  $r' = 3.5 - 6$  leads to find the pinch time nearer to the current peak (the pinch time tend to about 45-60 ns and the quarter current

period is 55 ns). This incidence happens as a result of Ohmic damping that brings about reduction in the current. In this case, compression happens later and nearer the current peak. Ultimately for having higher efficiency, we should reduce the resistance as much as possible.

All these results were provided in constant initial parameters, such as voltage, current peak, current period, pressure and capillary radius. Different value of these factors, bring about different situations for choosing proper value for the variable parts of the pumping system.

#### IV. CONCLUSION

Here we are looking for the best conditions to optimize the output efficiency and minimize the time interval between pinch time and current peak. It was investigated that for reducing the energy dissipation one should choose the right value for the capacitance, resistance and inductance of the pumping circuit, regarding to the fixed initial conditions. The optimum regions for all the circuit parameters were shown in the figures and they differ for the other conditions. Reducing the inductance and the resistance as much as possible (less than 1 in normalized value), choosing the normalized capacitance values between ( $\kappa = 0.2 - 0.7$ ), for the selected conditions, would be the best choices.

#### REFERENCES

- [1] D.D. Ryutov, M.S. Derzon, and M.K. Matzen, "The Z-pinch approach to fusion," *Rev. Mod. Phys.* Vol. 72, pp. 167-223, 2000.
- [2] M.G. Haines, S.V. Lebedev, J.P. Chittenden, F.N. Beg, S.N. Bland, and A.E. Dangor, "The past, present, and future of Z-pinchs," *Phys. Plasmas*, Vol. 7, pp. 1672-1681, 2000.
- [3] A.E. Dangor, "High density Z-pinchs," *Plasma Phys. and Control. Fusion*, Vol. 28, pp. 1931-1942, 1986.
- [4] J.J. Rocca, V. Shlyaptsev, F.G. Tomasel, O.D. Cortazar, D. Hartshorn, and J.L.A. Chilla, "Demonstration of a Discharge Pumped

- Table-Top Soft-X-Ray Laser,” *Phys. Rev. Lett.*, vol. 73, pp. 2192-2197, 1994.
- [5] Y. Liu, M. Seminario, F. G. Tomasel, C. Chang, J. J. Rocca, and D. T. Attwood, “Achievement of essentially full spatial coherence in a high-average-power soft-x-ray laser,” *Phys. Rev. A*, Vol. 63, pp. 033802-033805, 2001.
- [6] L.B. Da Silva, J.E. Trebes, S. Mrowka, T.W. Barbee, Jr., J. Brase, J.A. Koch, R.A. London, B.J. MacGowan, D.L. Matthews, D. Minyard, G. Stone, T. Yorkey, E. Anderson, D.T. Attwood, and D. Kern, “Demonstration of x-ray microscopy with an x-ray laser operating near the carbon K edge,” *Opt. Lett.* Vol. 17, pp. 754-756, 1992.
- [7] P. Celliers, T.W. Barbee Jr., R. Cauble, L.B. Da Silva, C.D. Decker, D.H. Kalantar, M.H. Key, R.A. London, J.C. Moreno, R. Snavely, J.E. Trebes, A.S. Wan, and F. Weber, “Probing High Density Plasmas with Soft X-Ray Lasers,” *Soc. Photo-Optical Instrumentation Engineers Soft X-Ray Lasers and Applications II*. pp. 3-14, 1997.
- [8] R. Cauble, L.B. Da Silva, T.W. Barbee, Jr., P. Celliers, J.C. Moreno, and A.S. Wan, “Micron-Resolution Radiography of Laser-Accelerated and X-Ray Heated Foils with an X-Ray Laser,” *Phys. Rev. Lett.* Vol. 74, pp. 3816–3819, 1995.
- [9] P. Jaeglé, S. Sebban, A. Carillon, G. Jamelot, A. Klisnick, P. Zeitoun, B. Rus, M. Nantel, F. Albert, and D. Ros, “Ultraviolet luminescence of CsI and CsCl excited by soft x-ray laser,” *J. Appl. Phys.* Vol. 81, pp. 2406-2409, 1997.
- [10] P. Vrba and M. Vrbova, “Z-Pinch Evolution in Capillary Discharge,” *Plasma Phys.* Vol. 40, pp. 581-595, 2000.
- [11] S.V. Kukhlevsky, J. Kaiser A Ritucci, G. Tomassetti, A. Reale, L. Palladino, I.Z. Kozma, F. Flora, L. Mezi, O. Samek, and M. Liška, “Study of plasma evolution in argon-filled capillary Z-pinch devoted to x-ray production,” *Plasma Sources Sci. Technol.* Vol. 10, pp. 567-572, 2001.
- [12] N.A. Krall and A.W. Trivelpiece, *Anomalous Penetration of a Magnetic Pulse into a Plasma*, Principles of Plasma Physics, McGraw-Hill, New York, 1973.
- [13] J. Katzenstein, “Analyzing time-resolved spectroscopic data from an azimuthally symmetric, aluminum-wire array, z-pinch implosion,” *J. Appl. Phys.* Vol. 52, pp. 676-681, 1981.
- [14] Y. Hayashi, H. Taniguchi, H. Ghomi, P. Chalise, N. Sakamoto, M. Watanabe, A. Okino, M. Nakajima, K. Horioka, and E. Hotta, “On the Amplification Capability of Ne-like Ar Soft X-ray Laser Generated by Capillary Z-Pinch Discharge,” *Jpn. J. Appl. Phys.*, Vol. 43, pp. 5564-5565, 2004.
- [15] Y. Hayashi, H. Ghomi, H. Taniguchi, N. Sakamoto, M. Watanabe, A. Okino, K. Horioka, and E. Hotta. “Operating Conditions of the Capillary Discharge for Soft X-Ray Laser Generation,” *Proc. 26th Int. Conf. on Phenomena in Ionized Gases*, Vol. 2, pp. 107-108, 2003.
- [16] Y. Hayashi, N. Sakamoto, Y. Zhao, Y. Cheng, P. Chalise, M. Watanabe, A. Okino, K. Horioka, and E. Hotta, “Influence of Z-pinch evolution on laser pulse duration at 46.9 nm in Ne-like Ar ions,” *Plasma Sources Sci. Technol.* Vol. 13, pp. 675-679, 2004.
- [17] J. Katzenstein, “Optimum coupling of imploding loads to pulse generators,” *J. Appl. Phys.* Vol. 52, pp.676-680, 1981.

THIS PAGE IS INTENTIONALLY LEFT BLANK.